

# Influence of Polyfunctional Monomer on Melt Strength and Rheology of Long-Chain Branched Polypropylene by Reactive Extrusion

Feng-Hua Su, Han-Xiong Huang

Center for Polymer Processing Equipment and Intellectualization, College of Mechanical and Automotive Engineering, South China University of Technology, Guangzhou 510641, People's Republic of China

Received 21 June 2009; accepted 6 November 2009

DOI 10.1002/app.31738

Published online 20 January 2010 in Wiley InterScience (www.interscience.wiley.com).

**ABSTRACT:** Long chain branching (LCB) were added to linear polypropylene (PP) using reactive extrusion in the presence of selected polyfunctional monomers (PFMs) and a peroxide of dibenzoyl peroxide (BPO). Fourier Transformed Infrared spectra (FTIR) directly confirmed the grafting reaction occurred during the reactive extrusion process. Various rheological plots including viscosity curve, storage modulus, Cole-Cole plot, and Van-Gurp plots, confirmed that the LCB structure were introduced into modified PPs skeleton after modification. In comparison with linear PP, the branched samples exhibited higher melt strength, lower melt flow index, and the enhancement of crystallization temperature. The LCB level in modified PPs and their melt strength were affected by the type of PFM used and could be controlled by the PFM

properties and structure. PFMs with lower boiling points, such as 1, 4-butanediol diacrylate (BDDA), could not produce LCB structure in modified PP skeleton. The shorter molecular chain bifunctional monomers, such as 1,6-hexanediol diacrylate (HDDA), favored the branching reaction if their boiling points were above the highest extrusion temperature. And some polar groups, such as hydroxyl, in the molecule of PFM were harmful to the branching reaction, which might be attributed to the harm of the polarity of groups to the dispersion of PFM in PP matrix. © 2010 Wiley Periodicals, Inc. *J Appl Polym Sci* 116: 2557–2565, 2010

**Key words:** long chain branching polypropylene; reactive extrusion process; rheology; melt strength; polyfunctional monomer

## INTRODUCTION

Polypropylene is one of the leading and fast growing thermoplastic polymers in the world because it has many desirable properties, such as high melting point, high tensile strength, stiffness, low density, and excellent chemical resistance. However, commercial PP produced via Ziegler-Natta or metallocene catalysts suffers from a low melt strength (MS) i.e., the melted PP does not exhibit an increase in resistance to stretching during elongation. The relatively low melt strength and exhibiting no strain hardening for commercial PPs limits their use in applications, such as thermoforming, blow molding, foaming, and extrusion coating. It is well known that the melt strength of a polymer has relation with its molecular structure. Long chain branching (LCB) can increase the entanglement level, thereby increase the melt strength as well.<sup>1–3</sup> The LCB structure can

improve the processing ability of PP under melt conditions, including strain hardening, shear thinning, etc., thus broadening the end uses and processing methods for PP.<sup>4–6</sup>

Therefore, different methods have been applied in the past to modify PP by long chain branching, and several commercial grades of LCB-PP with high melt strength are available. LCB-PPs are mostly produced by *in situ* polymerization<sup>7–9</sup> and post-reactor treatment<sup>1,2,10–20</sup> that included two methods i.e. electron beam irradiation<sup>11–14</sup> and reactive extrusion processes.<sup>2,15–20</sup> Compared with *in situ* polymerization and electron beam irradiation, the reactive extrusion has many merits, including simple operation, low cost, and high productivity. For this reason, the preparation of LCB-PP by reactive extrusion has generated increasing interest over the past decades. Legendijk et al.<sup>2</sup> achieved this objective by reactive extrusion in the presence of peroxydicarbonate with various structures. They found that all modified samples showed enhanced strain hardening, slightly lower melt flow index, increased extrudate swelling, and the improvement of melt strength. However, it is known that PP has a tendency to undergo  $\beta$ -scission because of the nature of its molecular structure, and this competes with grafting and cross-linking reactions process. A relatively low concentration of

Correspondence to: F.-H. Su (fhsu@scut.edu.cn).

Contract grant sponsor: National Natural Science Foundation of China; contract grant number: 20904012.

Contract grant sponsor: China Postdoctoral Special Science Foundation; contract grant number: 200902319.

TABLE I  
PFMs Used for Modification, Their Chemical Name, Molecular Structure and Boiling Point

Chemical name	Abridged name	Chemical formula	Mw (kg/mol)	Boiling point (°C)
1, 4-butanediol diacrylate	BDDA	$\text{CH}_2=\text{CHCOOCH}_2(\text{CH}_2)_2\text{CH}_2\text{OOCCH}=\text{CH}_2$	198	< 160
1, 6-hexanediol Diacrylate	HDDA	$\text{CH}_2=\text{CHCOOCH}_2(\text{CH}_2)_4\text{CH}_2\text{OOCCH}=\text{CH}_2$	226	>210
Pentaerythritol triacrylate	PETA	$(\text{CH}_2=\text{CHCOOCH}_2)_3-\text{CCH}_2\text{OH}$	298	>210
Trimethylol propane triacrylate	TMPTA	$(\text{CH}_2=\text{CHCOOCH}_2)_3-\text{CC H}_2\text{CH}_3$	296	>210

peroxide in the primary radical will abstract preferentially the tertiary hydrogens leading to the degradation of tertiary polypropylene macroradicals during the reactive extrusion process. The addition of polyfunctional monomers (PFMs) to the reaction system can decrease the degradation and improve the branching for PP because the monomer convert some of the tertiary macroradicals to the more stable secondary macroradicals that tend to undergo recombination rather than scission.<sup>15–17,19</sup> As for the preparation of the high melt strength PP via irradiation, the influence of PFM structure on the melt strength and the thermal behavior has been investigated by Yoshii et al.<sup>13</sup> They found that the relatively shorter molecular chain bifunctional monomers, such as BDDA and HDDA, were the most effective for enhancing the melt strength of PP modified with irradiation. However, to the best of authors' knowledge, the influences of the PFM properties and structure on the branching level and melt strength on modified PPs by reactive extrusion have not been reported till now.

The low frequency rheological response of a polymer is extremely sensitive to its molecular structure. Compared with NMR and GPC rheology is a more appropriate and reliable technique for verifying the existence of long branches on the polymeric chains.<sup>7,11,15,17,19,20–23</sup> García-Franco et al.<sup>21</sup> suggested that the level of LCB on polyethylene can be quantified by small amplitude oscillatory shear experiments, with analysis predicated on use of so-called Van Gurp-Palmen plots (Van-Gurp plots). Yu and coworkers<sup>15</sup> confirmed the LCB structure on modified PPs by small-amplitude oscillatory shear experiment and suggested a new method to determine the branching number on the basis of macromolecular dynamics models. Besides shear rheology, extensibility of the polymer melt is also sensitive to the LCB structure of polymer. The maximal drawdown force was deemed as "melt strength" during the extensile experiment of polymer melt, which can be determined by use of an "extension diagram".<sup>24,25</sup> Moreover, the main objective underlying the introduction of LCB onto a linear PP backbone is also to increase the melt strength and improve the processing ability for the linear PP.

In the present contribution, our efforts focused on the preparation of LCB-PP by reactive extrusion in the presence of various PFMs and a peroxide of dibenzoyl peroxide (BPO), and the influences of the PFM properties and structure on the LCB level and melt strength of modified PPs were systemically investigated with the help of oscillatory shear rheology and extensional flow behavior of polymer melt. Moreover, the contribution provides an expansion for the mechanism by which different PFMs cause the modification of melt strength and rheology.

## EXPERIMENTS

### Materials and sample preparation

The isotactic polypropylene was supplied in powder form by Maoming Petrochemical Corporation, China. The number average molecular weight ( $M_n$ ) was 57.992 g/mol, the weight average molecular weight ( $M_w$ ) was 386.786 g/mol and the polydispersity ( $M_w/M_n$ ) was 6.7. The PP powder was stabilized by the addition of 0.1 wt % Irganox 1010 (Jinhai Albemarle, China) antioxidant. Dibenzoyl peroxide (abridged as BPO) was purchased from Lanzhou Auxiliary Agent Plant. Various polyfunctional monomers (abridged as PFMs) were purchased from Tianjintianjiao Chemical Co, China. The chemical name, properties, and molecular structure of these are shown in Table I. The peroxide and PFMs were used as received.

For even dispersion of BPO and PFM in the PP powder, these were dissolved in 50 mL acetone, and this solution was added to 1000 g PP powder during mixing process. The concentrations of PFM and BPO relative to PP powder were fixed at  $1.2 \times 10^{-1}$  mol/kg and  $1.2 \times 10^{-3}$  mol/kg, respectively. The mixing of linear PP with antioxidant, BPO, and PFM in the SHR10A high speed mixer was maintained for 10 min and was followed by modification of the linear PP in a TE35 co-rotating twin-screw extruder with 35 mm diameter and 38 : 1 length-to-diameter ratio. The extruder has six heating zones, and the temperatures were maintained at 160°C, 180°C, 200°C, 200°C, 210°C, 210°C from hopper to die. The throughput and the screw speed were 4.8 kg/h and

**TABLE II**  
Composition of Peroxide and Polyfunctional Monomer Used for Modifying PP

Samples	BPO peroxide ( $1.2 \times 10^{-3}$ mol/kg)	PFM ( $1.2 \times 10^{-1}$ mol/kg)
PP1	–	–
PP2	+	BDDA
PP3	+	HDDA
PP4	+	PETA
PP5	+	TMPTA

60 rpm, respectively. During extruding process, a devolatilization zone was established before the pumping zone, close to the die, to remove small molecules, such as peroxide decomposition products and acetone. Extrudates were cooled in water and then pelletized. The initial PP and modified PPs with different PFMs in the presence of BPO are shown in Table II

### Characterization

#### FTIR

FTIR spectra of all samples were measured at room temperature using Bruker Tensor 27 Fourier transformation infrared spectroscope (FTIR). The modified PPs were added in xylene and then heated to 140°C. The solutions were then charged into acetone at room temperature. Unreacted monomer and copolymerized monomer remained soluble, while PP and grafted PPs precipitated out. The modified PPs were separated by filtration and then were dried at 80°C under vacuum for 48 h. The purified samples were pressed into films for FTIR analysis.

#### DSC

The crystallization temperatures of the initial and modified PPs were investigated by DSC204F1 differential scanning calorimetry (NETZSCH Co., Germany). Specimens were heated to 200°C at a rate of 10°C/min, held for 3 min to eliminate the thermal histories, and then cooled down to 25°C at a rate of 10°C/min to determine the crystallization temperature.

#### Melting flow rate

The melting flow properties of the initial and reacted PPs were measured by MFI tester CEAST 7072. The

measurements were carried out at 230°C using a load of 2.16 kg according to the GB3682 standard.

#### Rheology

The oscillatory shear rheology was conducted with a Bohlin Gemini 200 Rheometer equipped with a parallel-plate fixture (25 mm diameter). Disk samples were prepared by compression molding with a thickness of 2.0 mm and diameter of 25 mm. The gap between the two parallel plates was maintained at 1.75 mm for all measurements. Small-amplitude oscillatory shear tests were performed as a function of angular frequency ( $\omega$ ) ranging from 0.01 rad/s to 100 rad/s at 190°C. A fixed strain of 1% was used to ensure that measurements were carried out within the linear viscoelastic range of the materials investigated. Steady model measurements were conducted as a function of shear rate to determine the zero shear viscosity. At sufficiently low shear rate, the shear viscosity of the test sample becomes steady and is then independent of shear rate, allowing determination the zero shear viscosity, as follows:

$$\lim_{\dot{\gamma} \rightarrow 0} \eta(\dot{\gamma}) = \eta_0 \quad (1)$$

#### Melt strength

The melt strength was measured using a four-wheeled Göttfert Rheotens 71.97 tester in combination with Göttfert Rheograph 25 High Pressure Capillary Rheometer. The Rheotens 71.97 was located close to the exit of the capillary. The additional pair of pull-off wheels was integrated to prevent sticking of the elongated polymer strand once it had passed the first pair of pulleys during the test. Table III lists the settings that were used for testing the melt strength. Plastic pellets were melted in heated test cylinder and pressed with a test piston at a constant speed through a capillary. The melt strand was continuously drawn down at a linear exponentially accelerating velocity between the two counter-rotating wheels of the device, which were mounted on a balanced beam. The drawdown was continuously measured as a function of the angular speed of the wheels as the melt strand was pulling. The force when the melt strand was broken was deemed as “melt strength (Ms)” for the tested condition.

**TABLE III**  
Geometry and Operating Parameters for the Elongational Experiment (Rheotens) Used to Measure the Melt Strength

Capillary rheometer parameter			Rheotens 71.97 parameter
Die geometry	Length = 30 mm	Diameter = 1 mm	The gap between two wheels = 0.3 mm
Piston	Speed = 0.1 mm/s	Diameter = 15 mm	$V_0 = 20$ mm/s
Shear rate = $180 \text{ s}^{-1}$	Temperature = 180°C	Melt time = 30 min	Acceleration = $2.4 \text{ mm/s}^2$

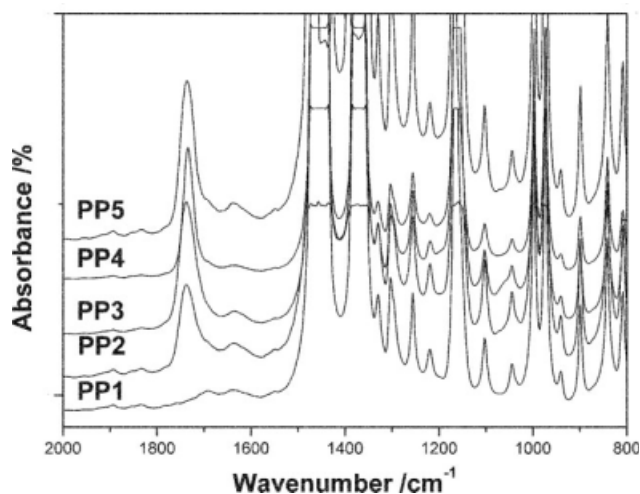


**Figure 1** FTIR spectra of initial and modified PPs with different PFMs in the presence of BPO.

## RESULTS AND DISCUSSION

### FTIR spectroscopy

Figure 1 shows the FTIR spectra of initial PP and modified PPs after purification. A band at about  $1735\text{ cm}^{-1}$  was found in all modified PPs, which was ascribed to the stretching vibration of carbonyl group of the ester in the PFM molecule, indicating that grafting reaction occurred<sup>15,16,20</sup> as PP modified with different PFMs in the presence of a peroxide of BPO. Meanwhile, it was found that the band intensity at  $1735\text{ cm}^{-1}$  was different for modified PPs with different PFMs in the presence of BPO. Not only the grafting degree but the number of ester group in each PFM could affect the band intensity at  $1735\text{ cm}^{-1}$ . Therefore, the band intensity at  $1735\text{ cm}^{-1}$  was unable to evaluate the grafting degree of different PFMs. The FTIR from Figure 1 confirmed the grafting reaction occurred as linear PP was modified with different PFMs in the presence of a peroxide of BPO but could not differentiate the structure of long-branched chains versus short-branched chains. The linear viscoelastic properties were sensitive to the LCB of the polymer, which were discussed in the subsequent section.

### Melt flow properties

The influences of the molecular structure on the melt flow index (MFI) of polymers have been studied extensively, and the MFI also decrease with increasing molecular weight or increasing LCBs for the same polymer.<sup>2</sup> In this research, the MFIs of initial PP and modified PPs are shown in Figure 2. It was seen that MFI of PP2 was slightly higher than that of the PP1, indicating that the degradation reaction was also serious as linear PP was modified with BDDA in the presence of BPO besides grafting reaction (see Fig. 1). The MFIs of PP3, PP4, and PP5

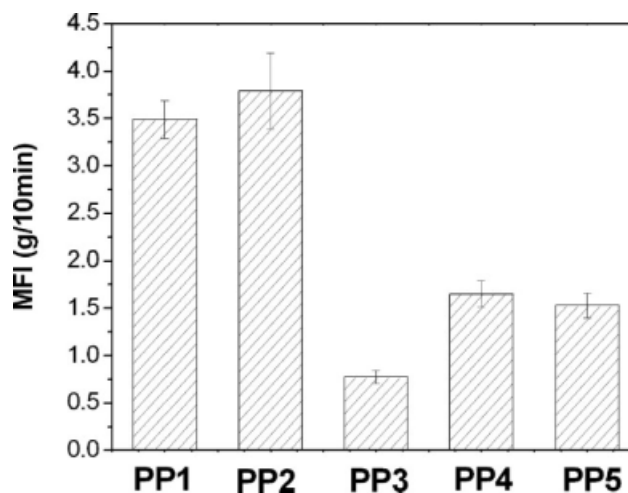


**Figure 2** Melt flow index (MFI) of initial PP and modified PPs with different PFMs in the presence of BPO.

were lower than that of PP1 indicating that the grafting reaction were dominant for these samples in comparison with degradation reaction resulting in the increase of their molecular weight. The MFI also changed with the type of PFM because of their different branching efficiencies. The PP modified with HDDA had the lowest MFI of all modified samples, which might be due to a large number of branched chains on its backbone.

### Crystallization temperature

The modification of PP with a peroxide and polyfunctional monomer will result in a change in the molecular weight and its distribution, and also in a change in chain irregularity. These variations in the microstructure affect the crystallization behavior of the system. Figure 3 shows the DSC cooling

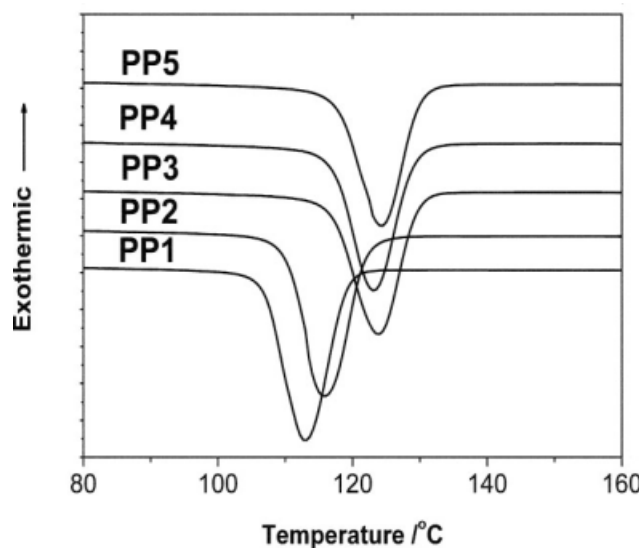


**Figure 3** DSC cooling thermograms of initial PP and modified PPs with different PFMs in the presence of BPO.



**TABLE IV**  
**Various Parameters for Initial PP and Modified PPs with Different PFMs in the Presence of BPO**

Sample	The terminal slope of $G'$	Crystallization temperature ( $^{\circ}\text{C}$ )	$\eta_0$ ( $\times 10^4$ Pa s)	Bn
PP1	1.62	112.7	0.68	–
PP2	1.51	116.2	0.71	–
PP3	0.79	124.0	1.96	0.80
PP4	1.24	123.2	1.16	0.40
PP5	1.07	124.2	1.24	0.46

thermograms of the initial PP and modified samples. The corresponding crystallization temperatures ( $T_c$ ) are shown in Table IV. The crystallization exotherm was an indication of the bulk crystallization rate. The degradation of linear PP lead to the enhanced molecular chain segment's mobility, which favored the diffusion and arrangement of macromolecules into crystal cell, therefore, the  $T_c$  increased for degraded PP.<sup>16</sup> At the same time, Tang et al.<sup>25</sup> had reported that the LCB structure could act as a nucleating agent for the crystallization of PP, which resulted in the higher  $T_c$  for branched PP. However, the enhanced level of  $T_c$  caused by degraded reaction was lower than that caused by LCB structure.<sup>16</sup> Although the grafting reaction occurred for PP2 (see Fig. 1), the grafting reaction had not produced LCB structure onto its backbone; moreover, the degradation reaction was serious. As a result, the crystallization temperature of PP2 was slightly higher than that PP1. However, the  $T_c$  of PP3, PP4, and PP5 was much higher than that PP1. It was inferred that the branching reaction was dominant in comparison with the degradation reaction for PP3, PP4, and PP5, resulting in a large number of LCB in their skeleton.

### Oscillatory shear rheology

The storage modulus was even more sensitive to long chain branched structure of PP.<sup>15</sup> The storage modulus ( $G'$ ) plotted as a function of sweeping frequency ( $\omega$ ) of initial PP and modified PPs is shown in Figure 4. PP1 exhibited the typical terminal behavior because of its linear chain structure. The typical terminal behavior was also observed in PP2, indicating no LCB structure existed in PP2 skeleton. As shown in Figure 1, the grafting reaction also occurred for PP2. Therefore, it could be inferred that only a few short branched chains had been grafted in PP2 skeleton that did not significantly affect its viscoelastical behavior. However, PP3, PP4, and PP5 deviated from the terminal behavior. And the  $G'$  of them are higher than that of initial PP1 at low frequency, and the terminal slopes decreased from 1.62 for linear PP1 to 0.79 for PP3, 1.24 for PP4 and 1.07 for PP5 (see Table IV). This result was attributed to

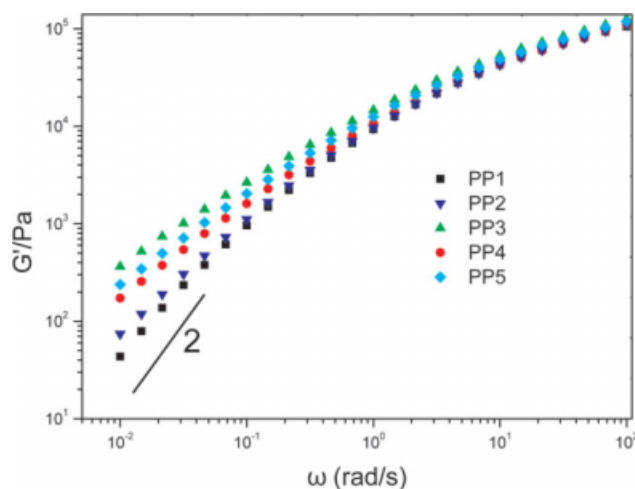


**Figure 4**  $G'$  vs.  $\omega$  of initial PP and modified PPs with different PFMs in the presence of BPO at  $190^{\circ}\text{C}$ . [Color figure can be viewed in the online issue, which is available at [www.interscience.wiley.com](http://www.interscience.wiley.com).]

the form of the long branched chain in their skeleton leading to the increased dynamic modulus at low frequency and the longer relaxation time.<sup>15</sup> Moreover, it was obvious that the curves and the terminal slopes of modified PPs varied with the type of PFM used for modification, suggesting that the elastic response and the level of LCB in modified PPs were affected by the structure and property of the PFM. Comparison of these curves indicated that best branching efficiency was obtained with HDDA, followed by TMPTA and then PETA.

The degree of shear thinning increased as amounts of LCB on PP backbone in comparison with linear PP with similar molecular weight.<sup>15,17,19</sup> The complex viscosity ( $\eta^*$ ) versus sweeping frequency ( $\omega$ ) of initial PP and modified PPs are shown in Figure 5.

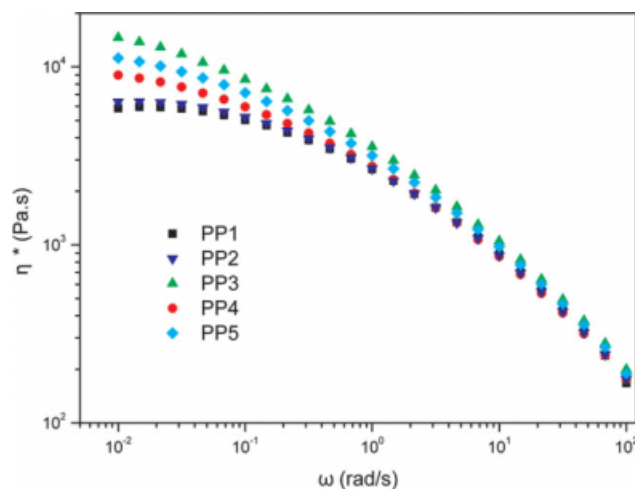


**Figure 5**  $\eta^*$  vs.  $\omega$  of initial PP and modified PPs with different PFMs in the presence of BPO at  $190^{\circ}\text{C}$ . [Color figure can be viewed in the online issue, which is available at [www.interscience.wiley.com](http://www.interscience.wiley.com).]

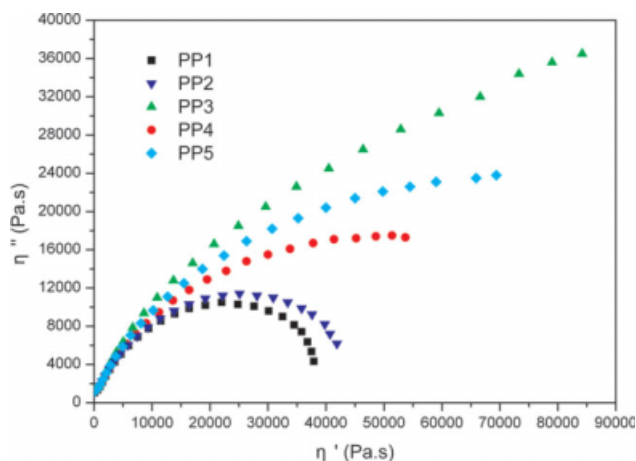


**Figure 6** Cole-Cole plot of initial PP and modified PPs with different PFMs in the presence of BPO at 190°C. [Color figure can be viewed in the online issue, which is available at [www.interscience.wiley.com](http://www.interscience.wiley.com).]

The curves of PP1 and PP2 exhibited the presence of a plateau at low frequency, which was because of their linear molecular structure. The  $\eta^*$  increased at low frequency and the behavior of shear-thinning increased for PP3, PP4, and PP5, which was attributed to the existence of LCB in their skeleton. Moreover, it was seen that the behavior of shear-thinning varied with the type of PFM. The shear-thinning behavior of PP modified with HDDA was the most distinct among all investigated cases, indicating a large number of LCBs were grafted in its skeleton.

The relaxation process can be estimated by a Cole-Cole plot ( $\eta''$ - $\eta'$ ).<sup>15</sup> A semicircle Cole-Cole plot of a polymer indicated the chain structure of the polymer is linear. Moreover, a higher molecular weight results in an increased radius of the semicircle. Figure 6 shows the Cole-Cole plots of initial PP and modified PPs. The Cole-Cole plot of PP1 exhibited almost the semicircle because of its linear chain structure. The Cole-Cole plot of PP2 also exhibited almost the semicircle, indicating that its molecular structure was linear. Surprisingly, the radius of the semicircle for PP2 was bigger than that for PP1, indicating that the molecular weight of PP2 was bigger than that of PP1. Therefore, it could be inferred that the grafting reaction resulted in many short chains grafted on PP2 skeleton although the degradation reaction also occurred for PP2. The Cole-Cole plots of PP3, PP4, and PP5 were higher than that of PP1 and showed more evident upturning at high viscosity, indicating that these samples had longer relaxation times. Therefore, it could be inferred that a large number of LCBs were indeed introduced onto PP3, PP4, and PP5 skeleton, especially for PP3.

The Van-Gurp plot has been used to get an insight into long-chain branching in polymer chain.<sup>11,21-23</sup> Auhl et al.<sup>11</sup> suggested that the phase angle toward

smaller values at fixed  $G^*$  was caused by an introduction of long-chain branching in PP. The same method was also used in the present work for assessing the existence and the level of LCB in these modified samples. As shown in Figure 7, the similar Van-Gurp plots for PP1 and PP2 further indicated no LCB in PP2 skeleton. However, the Van-Gurp plots of PP3, PP4, and PP5 shifted to smaller values of the phase angle in comparison with PP1, indicating that the PFMs of HDDA, TMPTA, and PETA did produce LCB in PP skeleton during the reactive extrusion process in the presence of BPO. The shifting of Van-Gurp plots to smaller values of phase angle varied with the type of PFM, suggesting that the branching efficiency of various PFMs was dissimilar in our research system. The shifting of Van-Gurp plots indicated the LCB amounts in modified PPs were as follows: PP3 > PP5 > PP4. This also suggested that the branching efficiency of PFM used for modification was as follows: HDDA > TMPTA > PETA.

#### Analysis of branching number

Figure 8 shows the shear viscosity ( $\eta$ ) of the initial PP and modified PPs as a function of shear rate ( $\dot{\gamma}$ ). As illustrated in the experimental section, the zero shear viscosity ( $\eta_0$ ) can be obtained from Figure 8, and the values are listed in Table IV. Tsenoglou and Gotsis<sup>26</sup> have tried to determine the level of LCB in modified PPs with peroxydicarbonates. They assumed that the linear polymer chain break through scission and some of their fragments cross-linked with neighbors to form the three-arm branched molecules. The reacted product was a blend consisting of linear molecular and three-arm

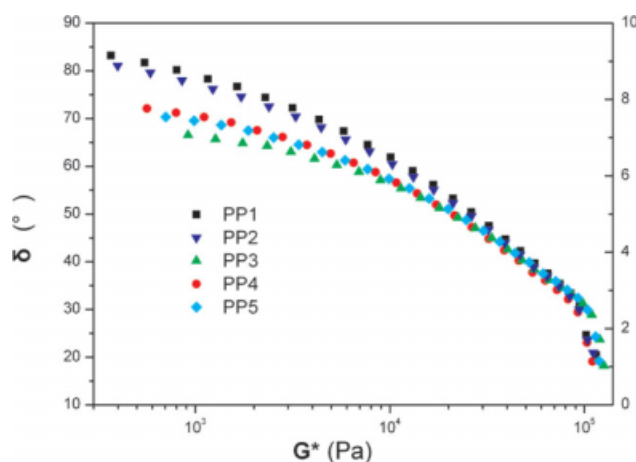


**Figure 7** The Van-Gurp plot of initial PP and modified PPs with different PFMs in the presence of BPO at 190°C. [Color figure can be viewed in the online issue, which is available at [www.interscience.wiley.com](http://www.interscience.wiley.com).]

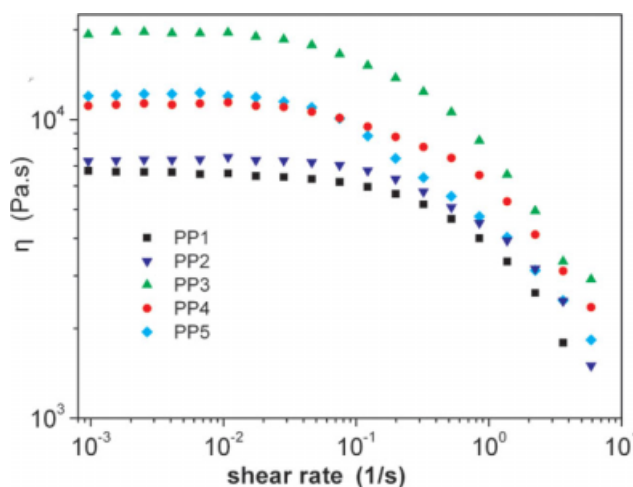


**Figure 8**  $\eta$  vs.  $\dot{\gamma}$  of initial PP and modified PPs with different PFM in the presence of BPO at 190°C. [Color figure can be viewed in the online issue, which is available at [www.interscience.wiley.com](http://www.interscience.wiley.com).]

branched molecules. The weight fractions of branched chains can be expressed as follows:

$$Bn = \frac{\ln(\eta_{BL}/\eta_L)}{\alpha(M_L/M_C) - 3 \ln(M_L/M_C)} \quad (2)$$

where,  $\eta_{BL}$  is the zero-shear viscosity of branched linear blend,  $\eta_L$  and  $M_L$  are the zero-shear viscosity and the weight average molecular weight of the linear precursor and  $\alpha$  is an adjustable parameter ( $\alpha = 0.42$ ).  $M_C$  is the molecular weight between two successive entanglements and is roughly equal to 11.2 kg/mol for PP. To obtain the value of  $Bn$ ,  $M_L$  is calculated from the relationship between  $\eta_0$  and  $M_w$  of the linear PP, as follows:

$$\text{Log } \eta_0 = -15.4 + 3.5 \text{ log } M_w \quad (3)$$

It is clear that eq. (2) can be used only when  $\eta_{BL}$  is higher than that  $\eta_L$ . No obvious difference of the zero-shear viscosity for PP1 and PP2 was observed, which lead to the branching number of PP2 could not be calculated. The result suggested that BDDA nearly could not produce LCB onto PP backbone. Other values of branching number ( $Bn$ ) for PPs modified with different PFM in presence of BPO are predicated by eq. (2) and are listed in Table IV. It was evident that the branching number was different for different PFM modified PPs. The PP modified with HDDA had the highest branching efficiency, followed by TMPTA and then PETA (Table IV). Actually, a very crude approximation has been made when deriving eq. (2), assuming that the breakage of the linear chain occurs in the middle and this result in the branched chains of arm molec-

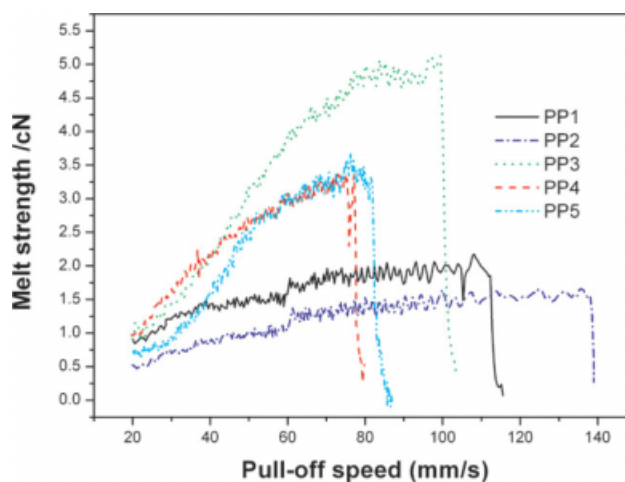


**Figure 9** Rheotens curves (draw down force as a function of the draw speed) of initial PP and modified PPs with different PFMs in the presence of BPO at 180°C. [Color figure can be viewed in the online issue, which is available at [www.interscience.wiley.com](http://www.interscience.wiley.com).]

ular mass. The LCB can enhance the melt strength of PP, inversely; the branching level can be indicated with the value of melt strength.

### Melt strength

The Rheotens curves i.e. the drawdown force versus draw speed of PP1 and modified PPs are show in Figure 9. The force when the melt strand was broken was deemed as “melt strength ( $M_s$ )” at the tested condition. Comparisons of the melt strength ( $M_s$ ), branching number ( $Bn$ ), and melt flow index (MFI), of the PP1 and modified PPs are shown in Figure 10. As shown in Figures 9 and 10, the melt strength of PP2 was lower than that of PP1. This result might be attributed no LCB were grafted in PP2 skeleton and the degradation reaction also occurred during the reactive extrusion process. Unsurprisingly, the melt strengths of PP3, PP4, and PP5 were higher than that

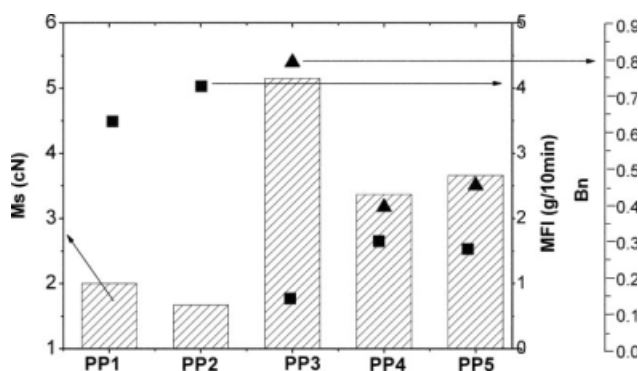


**Figure 10** Comparisons of the melt strength ( $M_s$ ), melt flow index (MFI) and branching number ( $Bn$ ) of initial PP and modified PPs with different PFMs in the presence of BPO.



of PP1. The melt strength of PP can be improved by increasing the molecular mass, broadening the distribution or by introducing branches. In the present research system, a peroxide and PFMs were used to modify PP. Therefore, it could be inferred that the improved melt strength of the modified PPs was indeed caused by the introduction of LCB structure. The values of melt strength of modified samples were affected by the level of LCB. PPs modified with HDDA, TMPTA, and PETA in the presence of BPO showed significant improvement in melt strength in comparison with PP1, which resulted from a larger number of LCBs in their backbone. PP modified with HDDA had the highest melt strength, followed by PP modified with TMPTA and then PETA.

As illustrated above, the MFI also decreased with increasing molecular weight or increasing LCB level for the same polymer. Figure 10 showed that the MFI decreased in general as LCB was grafted on PP skeleton, indicating the decrease of MFI for modified PPs was truly caused by the introduction of LCB in their skeleton. Meanwhile, it can be observed that the improved degree in melt strength was directly proportional to the branching number for modified samples, which again confirm that the improvement in melt strength was caused by the introduction of LCB onto their backbone. Modifications that result in more branches per chain also result in higher melt strength. But, the melt strength, branching number and melt flow index varied with the type of PFM used for modification, which might be attributed to the difference of the molecular structure and property of different PFMs, which was discussed in subsequent section.

## DISCUSSION

Yoshii et al.<sup>13</sup> had reported that the relatively shorter molecular chain bifunctional monomers such as BDDA and HDDA were the most effective for enhancing the melt strength of PP modified with irradiation in comparison with trifunctional monomer with longer molecular chain. However, their report is not absolutely right for the present research system because the modification of PP in the present research was conducted by reactive extrusion maintained at 160–210°C in extruder. Although the bifunctional monomer of BDDA had shorter molecular chain, the boiling point of it (132–134°C) was very low. The low boiling point of BDDA might prevent the long-time grafting reaction between PP and BDDA because of the gasification of BDDA before PP being completely melted. Comparison of trifunctional monomer of TMPTA and PETA, the branching degree of HDDA was more effective that resulted in PP3 with highest melt strength and largest LCB in

its skeleton. The result might be because the shorter chain of HDDA penetrated well into PP chain and reacted effectively with PP chain in extruder. The molecular weight and molecular chain length of PETA and TMPTA were almost the same; however, the branching efficiency of TMPTA was better than that of PETA. From the molecular formula in Table I, it was seen that the molecule of PETA contain the group of hydroxyl (—OH). The hydroxyl in the molecule of PETA might affect the dispersion of PETA in the PP matrix, which would decrease the reaction probability between PP matrix and PETA. Therefore, the branching degree of modified PP with PTEA was lower than that of PP modified with TMPTA. In general, the results in the present work indicated that the PFM with too low boiling point, such as BDDA, could not introduce LCB into modified PP skeleton. The shorter molecular chain bifunctional monomers, such as HDDA, favored the branching reaction during the reactive extrusion process as its boiling point was above the highest extrusion temperature. Some polar groups, such as hydroxyl, in the molecule of PFM were harmful to the branching reaction, which might be attributed to the harm of the polarity of groups to the dispersion of PFM in PP matrix.

## CONCLUSIONS

In this study, LCB-PPs were prepared by a melt grafting reaction in the presence of polyfunctional monomer (PFM) and a peroxide of BPO. FTIR measurements directly confirmed the grafting reaction between different PFMs and PP matrix in the presence of a peroxide. DSC results showed that the crystallization temperatures of modified PPs with some selected PFMs were much higher than that of initial PP, which might be attributed to the introduction of LCB in their skeleton. The degree of branching could be estimated from the rheological properties and the value of the melt strength of these samples. The improved degree in melt strength was directly proportional to the LCB level for modified PPs. However, the MFI decreased with the increase of the LCB level.

The degree of long chain branching and the melt strength of modified PPs varied with the type of PFM in the presence of a peroxide of BPO. Based on the rheology and melt strength of modified PPs, it was concluded that branching efficiencies of the investigated PFMs were as follows: HDDA>TMPTA>PETA>BDDA. BDDA nearly could not introduce LCB onto linear PP backbone because of its low boiling point. The shorter molecular chain bifunctional monomers, such as HDDA, favored the branching reaction if its boiling point was above the highest extrusion temperature. And some polar



groups, such as hydroxyl, in the molecule of PFM was harmful to the branching reaction because the polarity of these groups harmed the dispersion of PFM in PP matrix.

### References

1. He, C. X.; Costeux, S.; Wood-Adams, P.; Dealy, J. H. *Polymer* 2003, 44, 7187.
2. Lagendijk, R. P.; Hogt, A. H.; Buijtenhuijs, A.; Gotsis, A. D. *Polymer* 2001, 42, 10035.
3. Gotiss, A. D.; Zeevenhoven, B. L. F. *Polym Eng Sci* 2004, 44, 973.
4. Park, C. B.; Cheung, L. K. *Polym Eng Sci* 1997, 37, 1.
5. Liu, C. S.; Wei, D. F.; Zheng, A. N.; Li, Y.; Xiao, H. N. *J Appl Polym Sci* 2006, 101, 4114.
6. Nam, G. J.; Yoo, J. H.; Lee, J. W. *J Appl Polym Sci* 2005, 96, 1793.
7. Weng, W.; Hu, W.; Dekmerzian, A. H.; Ruff, C. J. *Macromolecules* 2002, 35, 3838.
8. Shiono, T.; Azad, S. M.; Ikeda, T. *Macromolecules* 1999, 32, 5723.
9. Ye, Z.; Alobaidi, F.; Zhu, S. *Ind Eng Chem Res* 2004, 43, 2860.
10. Bing, L.; Chung, T. C. *Macromolecules* 1999, 32, 8678.
11. Auhl, D.; Stange, J.; Münstedt, H. *Macromolecules* 2004, 37, 9465.
12. Scheve, B. J.; Mayfield, J. W.; Denicola, A. J. Jr. U.S. Pat. 4,916,198, (1990).
13. Yoshii, F.; Makuuchi, K.; Kikukawa, S. *J Appl Polym Sci* 1996, 60, 617.
14. Krause, B.; Stephan, M.; Volkland, S.; Voigt, D.; Häußler, L.; Dorschner, H. *J Appl Polym Sci* 2005, 99, 250.
15. Tian, J. H.; Yu, W.; Zhou, C. X. *Polymer* 2006, 47, 7962.
16. Wang, X. C.; Tzoganakis, C.; Rempel, G. L. *J Appl Polym Sci* 1996, 61, 1395.
17. Graebing, D. *Macromolecules* 2002, 35, 4602.
18. Cassagnau, P.; Bounor-Legaré, V.; Fenouillot, F. *Int Polym Proc* 2007, 3, 218.
19. Wong, B.; Bakert, W. E. *Polymer* 1997, 38, 2781.
20. Su, F. H.; Huang, H. X. *J Appl Polym Sci* 2009, 113, 2126.
21. García-Franco, C. A.; Lohse, D. J.; Robertson, C. G.; Georjon, O. *Eur Polym J* 2008, 44, 376.
22. Larson, R. G. *The structure and Rheology of Complex Fluids*; Oxford University Press: Wellington, New Zealand, 1998.
23. Trinkle, S.; Walter, P.; Friedrich, C. *Rheol Acta* 2000, 39, 97.
24. Yoshi, F. *J Appl Polym Sci* 1997, 60, 617.
25. Tang, H. X.; Dai, W. N.; Chen, B. Q. *Polym Eng Sci* 2008, 48, 1339.
26. Tsenoglou, C. J.; Gotsis, A. D. *Macromolecules* 2001, 34, 4685.